Optimization and Engineering
https://doi.org/10.1007/s11081-026-10089-2

RESEARCH ARTICLE

Relax-and-round strategies for solving the unit commitment problem with AC power flow constraints

Dolores Gómez[1,2] · Simone Göttlich[3] · Alfredo Ríos-Alborés[1,2] · Pilar Salgado[1,2]

Received: 6 February 2025 / Revised: 22 January 2026 / Accepted: 9 February 2026

Abstract
The Unit Commitment problem with AC power flow constraints (UC-ACOPF) is a non-convex mixed-integer nonlinear programming (MINLP) problem encountered in power systems. Its combinatorial complexity, together with its non-convex and nonlinear constraints, makes it particularly challenging. A common approach to tackle this problem is to relax the integrality condition, but this often results in infeasible solutions. Consequently, rounding heuristics are frequently employed to restore integer feasibility. This paper addresses recent advances in heuristics aimed at quickly obtaining feasible points for the UC-ACOPF problem, focusing specifically on direct relax-and-round strategies. We propose a model-based heuristic that rescales the solution of the integer-relaxed problem before rounding. Furthermore, we introduce rounding formulas designed to enforce combinatorial constraints and with the aim of maintaining AC feasibility in the returned points. These methodologies are compared with standard direct rounding techniques in the literature, and applied to 6- and 118-bus test systems. Additionally, we integrate the proposed heuristics into an implementation of the Feasibility Pump (FP) method, demonstrating their utility and potential to enhance existing rounding strategies.

Keywords Unit commitment problem · Mixed-integer nonlinear programming · Heuristics · Numerical simulations

Mathematics Subject Classification 90B10 · 90C11 · 90C59

✉ Simone Göttlich
goettlich@uni-mannheim.de

1 Universidade de Santiago de Compostela, Departamento de Matemática Aplicada, Santiago de Compostela 15782, Spain

2 Galician Centre for Mathematical Research and Technology (CITMAga), Santiago de Compostela 15782, Spain

3 University of Mannheim, School of Business Informatics and Mathematics, 68159 Mannheim, Germany

Published online: 16 April 2026

1 Introduction

The Unit Commitment (UC) problem is a fundamental optimization task in managing and planning the operation of power grids. It aims to determine an optimal schedule for the operation of power plants that ensures the generation meets demand, complying with the technical and operational constraints of the different power generation technologies, as well as with the transmission characteristics of the grid (Padhy 2004). Over the years, the UC problem evolved in response to different paradigms of the power market, transitioning from centralized to competitive markets, and adapting to changes in the energy mix, which now, for example, includes a growing share of renewable energy sources alongside traditional coal, gas, hydro and nuclear power plants. Furthermore, the UC problem can be used as a short-term real-time tool (Li et al. 2024), or as a long-term planner (Zhang et al. 2023), but generally it is used as a day-ahead scheduler.

The large size of real power grids, the combinatorial nature of the UC problem, the uncertainty in some input data, and the non-convexity and non-linearity of certain grid representations present significant challenges. Therefore, the UC problem is often simplified based on the specific goals of the study. Various approaches have been used to tackle the UC problem, including reformulations (Chen et al. 2019; Yang et al. 2014; Ostrowski et al. 2011), relaxation and/or decomposition techniques (e.g., semi-definite programming (Bai and Wei 2009), Lagrange Relaxation (Murillo-Sanchez and Thomas 2000), Benders' Decomposition (Nick et al. 2015), Outer Approximation (Castillo et al. 2016)), heuristic methods (Senjyu et al. 2003), or machine learning (Xavier et al. 2021). Improving the efficiency of MILP formulations for this problem remains an open area of research (Tejada-Arango et al. 2019a). However, relying solely on linear grid representations for power grids can lead to additional costs due to uplift payments (Sauer 2014) or even security issues in highly constrained grids (Bai et al. 2015). This has motivated efforts to develop convex relaxations approaches for the AC power flow equations, providing more tractable formulations such as convex second-order conic relaxations (Bai et al. 2015; Liu et al. 2018; Tuncer and Kocuk 2022). The works (Montero et al. 2022) and (Aharwar et al. 2023) are recent reviews on the general UC problem and different stochastic modeling frameworks, respectively.

As the combinatorial nature of the UC problem is the main challenge, a natural approach is to relax the integrality condition on binary variables. State-of-the-art methods often rely on branch-and-cut solvers, where integer relaxation is integrated into the algorithm Belotti et al. (2013). For MILP formulations, the work (Wuijts et al. 2024) empirically concludes that relaxed approximations can yield significant computational time savings with minimal loss of solution quality. However, when the integrality condition is relaxed, the resulting solutions are often infeasible for the original problem. To restore integer feasibility, rigorous iterative methods (e. g. branching or rounding heuristics) need to be employed.

In the literature, rounding is a simple yet useful technique often applied directly by using a basic threshold, or through more advanced strategies involving optimization and iterative algorithms. These heuristics do not guarantee general feasibility or optimality for the original problem. In the latter category, the Feasibility Pump (Fischetti et al. 2005) and local integer search methods, such as Variable Neighborhood Search

(Lazić 2016), along with their variants, are popular choices for relax-and-round strategies in mixed-integer programming (MIP), including UC problems (Li et al. 2024; Ma et al. 2020). However, direct rounding techniques are also employed as straightforward strategies to ensure integer feasibility. In stochastic problems, different scenarios are often considered, and the weighted average commitment is simply rounded, as in Carøe and Schultz (1998). This approach is also common in the context of machine learning, where the average commitment is interpreted as a confidence level after the training stage Gao et al. (2024). Direct rounding is frequently used as a heuristic to enhance the convergence rate of progressive hedging algorithms (Ordoudis et al. 2015). Procedures involving relaxation approaches usually rely on rounding at some stage to ensure the integrality of the solution (Wu et al. 2023), Kjeldsen and Chiarandini (2012). Moreover, direct rounding heuristics can be more sophisticated, aiming to avoid combinatorial infeasibility related to other constraints, such as the minimum up/down time constraints Yang et al. (2014), Bai and Wei (2009).

In this paper, we propose novel relax-and-round approaches involving rounding formulas for the deterministic Unit Commitment problem with AC power flow constraints (UC-ACOPF), considering thermal power plants. First, we introduce a rescaling technique for the integrality-relaxed solution. It consists of a model-based heuristic aiming to improve the efficiency of other existing rounding methods. A rounding formula for a relax-and-round direct approach is also proposed. The new heuristics are compared with other rounding techniques from the literature and validated using two established benchmarks: the 6-bus test system and a modified IEEE 118-bus system. Finally, the efficiency of the rescaling technique on other rounding heuristics is tested by integrating them into a Feasibility Pump algorithm. The paper is organized as follows: Section 2 introduces the Unit Commitment problem. In Section 3, we present direct relax-and-round heuristics, followed by a discussion of their numerical results in Section 4. Section 5 covers the implementation of a Feasibility Pump algorithm combined with our proposed relax-and-round heuristics, along with the corresponding numerical results.

2 The UC-ACOPF problem

In this section, we introduce the mathematical framework of the Unit Commitment Problem with AC Power Flow Constraints (UC-ACOPF), a unified model for its formulation and solution.

The power grid is modeled as a directed graph $\mathcal{P} = (I, L)$, where the nodes $I = \{1, \ldots, N_\mathrm{b}\}$ represents buses, the edges $L \subset I \times I$ represent the N_l elements (e.g., transmission lines, transformers), and $l = (i, k)$ indicates that i and k are connected neighbors in $\mathcal{P}$. The neighbors of node i are denoted by $\mathcal{N}(i)$, and linear relations are expressed using the incidence matrix $\mathcal{A} := (a_{kl}) \in \mathcal{M}_{N_\mathrm{b} \times N_\mathrm{l}}$

$$a_{kl} = \begin{cases} 0, & \text{if node } k \text{ does not belong to line } l, \\ -1, & \text{if node } k \text{ is the 'from' node of line } l, \\ 1, & \text{if node } k \text{ is the 'to' node of line } l. \end{cases}$$

We define auxiliary matrices $C_1 := \left(c_{1,lk}\right) \in \mathcal{M}_{N_\mathrm{l} \times N_\mathrm{b}}$, where $c_{1,lk} = \max\{0, -a_{kl}\}$, and $C_2 := \left(c_{2,lk}\right) \in \mathcal{M}_{N_\mathrm{l} \times N_\mathrm{b}}$, where $c_{2,lk} = \max\{0, a_{kl}\}$. Generation units $g \in G = \{1, \ldots, N_\mathrm{g}\}$ are placed at specific nodes, with $G_i \subset G$ and $G_r \subset G$ denoting the subset of generation units placed at node $i \in I$ and region $r \in R$, respectively. Starting from an initial time t_0 with known initial conditions, the system evolves over discrete time steps $T = \{t_1, \ldots, t_f\}$, with known active $(P^D_{i,t})$ and reactive $(Q^D_{i,t})$ power demands at buses $i \in I_D \subset I$, for $t \in T$.

The UC problem is classically formulated as a mixed-integer linear problem, where the linear constraints account for the plant on/off status, ramping limits, minimum up/down times, and power generation limits, which together form the 'Unit Commitment skeleton'. A global linear power balance equation is usually included. This work extends the classical framework by incorporating AC Power Flow (ACPF) equations, which add nonlinear constraints related to active and reactive power balances at each bus and transmission line limits. Feasibility is evaluated based on whether the decision variables satisfy the UC skeleton, the ACPF constraints, or both. In the following, we will refer to edges as lines, and even though some of these may include other elements (transformers, etc) all components will be modeled using the same linear circuit, the so-called π model Zimmerman and Murillo-Sánchez (2020). Similarly, we will use the terms nodes and buses indistinctly. We define $\boldsymbol{x}$ as the vector of continuous decision variables and $\boldsymbol{y}$ as the vector of binary variables, with the pair $(\boldsymbol{x}, \boldsymbol{y})$ representing a point in the UC-ACOPF decision space.

2.1 Unit Commitment skeleton

For simplicity, we consider only thermal power plants, $g \in G_\mathrm{th} \subset G$, and synchronous condensers for reactive power compensation, $g \in G_\mathrm{sc} \subset G$, although other generation types, such as nuclear and renewable units, could be included. There are several formulations for modeling UC skeleton constraints, each with advantages in computational efficiency Carrión and Arroyo (2006), Ostrowski et al. (2011), Morales-España et al. (2013). In this work, we prioritize the feasibility properties of the returned solutions and adopt a combination of the approaches in Liu et al. (2018) and Constante-Flores et al. (2022). For each thermal generation unit $g \in G_\mathrm{th}$ and time $t \in T$, the decision variables include the on/off status, the switching-on and switching-off decisions, denoted by the binary variables $u_{g,t}, v_{g,t}$, and $w_{g,t} \in \{0, 1\}$, respectively, and the active and reactive power, $P^\mathrm{G}_{g,t} \in \{0\} \cup [P_{\min,g}, P_{\max,g}]$ and $Q^\mathrm{G}_{g,t} \in \{0\} \cup [Q_{\min,g}, Q_{\max,g}]$, respectively. The total power system cost function depends on active power generation and on/off scheduling decisions and is given by:

$$f_\mathrm{UC}(\boldsymbol{x}, \boldsymbol{y}) = \sum_{t \in T} \sum_{g \in G_\mathrm{th}} a_{g,2} \left(P^\mathrm{G}_{g,t}\right)^2 + a_{g,1} P^\mathrm{G}_{g,t} + a_{g,0} u_{g,t} + c_{g,u} v_{g,t} + c_{g,d} w_{g,t}. \quad (1)$$

The UC problem aims to minimize (1) subjected to the operation linear constraints presented next. The on/off status of each thermal unit $g \in G_\mathrm{th}$ follows combinatorial

constraints ensuring consistency across time steps

$$u_{g,t-1} - u_{g,t} + v_{g,t} - w_{g,t} = 0, \quad t \in T. \tag{2}$$

Minimum up/down time constraints

$$\sum_{\tilde{t}=t-T_g^u+1}^{t} v_{g,\tilde{t}} \leq u_{g,t}, \quad t \in \{T_g^u, \ldots, t_f\}, \tag{3}$$

$$\sum_{\tilde{t}=t-T_g^d+1}^{t} w_{g,\tilde{t}} \leq 1 - u_{g,t}, \quad t \in \{T_g^d, \ldots, t_f\}, \tag{4}$$

enforce that a unit remains on/off for at least T_g^u or T_g^d hours after a start-up or shut-down decision, respectively. Additionally, for every region $r \in R$ and time $t \in T$, thermal units must meet the active power reserve requirement, $P_{r,t}^{\text{res}}$, with individual reserves $P_{g,t}^{\text{res}} \in [0, P_{\max,g} - P_{\min,g}]$. The active power reserve requirement constraints are given by the linear inequalities:

$$\sum_{g \in G_r} P_{g,t}^{\text{res}} \geq P_{r,t}^{\text{res}}. \tag{5}$$

For simplicity, we assume a single region r in the power grid. For each synchronous condenser $g \in G_{\text{sc}}$, the reactive power $Q_{g,t}^{\text{G}}$ is constrained by

$$Q_{\min,g} \leq Q_{g,t}^{\text{G}} \leq Q_{\max,g}, \tag{6}$$

ensuring it remains within the specified operational limits. We also impose mixed-integer linear constraints that relate binary and continuous decision variables. For each $g \in G_{\text{th}}$ and $t \in T$, the ramping-up and down constraints for the active power generation are given by

$$P_{g,t}^{\text{G}} + P_{g,t}^{\text{res}} - P_{g,t-1}^{\text{G}} \leq R_g^u u_{g,t-1} + S_g^u v_{g,t}, \tag{7}$$

$$P_{g,t-1}^{\text{G}} - P_{g,t}^{\text{G}} \leq R_g^d u_{g,t} + S_g^d w_{g,t}. \tag{8}$$

These constraints ensure that power changes between consecutive time steps respect the ramping up/down, R_g^u, R_g^d, limits, which prevent abrupt variations in power generation, while also accounting for the power generation limits, S_g^u, S_g^d, after starting-up and before shutting down. Also, we consider the general power generation limits

$$P_{\min,g} u_{g,t} \leq P_{g,t}^{\text{G}}, \quad P_{g,t}^{\text{G}} + P_{g,t}^{\text{res}} \leq P_{\max,g} u_{g,t}, \tag{9}$$

$$Q_{\min,g} u_{g,t} \leq Q_{g,t}^{\text{G}} \leq Q_{\max,g} u_{g,t}. \tag{10}$$

Usually, $P_{\min,g} > 0$, and then the generator's power output transitions from 0 (off state) to the operating range $[P_{\min,g}, P_{\max,g}]$ depend on the binary variable $u_{g,t}$. In contrast, $Q_{\min,g}$ is usually zero or negative (symmetrical situation for $Q_{\max,g}$), making $Q^{\mathrm{G}}_{g,t}$ a continuous variable over $[Q_{\min,g}, Q_{\max,g}]$. This inconvenient discontinuity in $P^{\mathrm{G}}_{g,t}$ Atakan et al. (2017)) can be mitigated by redefining it into two mixed-integer components, $P^{\mathrm{G}}_{g,t} = P_{\min,g} u_{g,t} + p^{\Delta}_{g,t}$, with $p^{\Delta}_{g,t} \in [0, P_{\max,g} - P_{\min,g}]$.

2.2 AC power flow equations

The ACPF model equations vary depending on the chosen representation of the complex variables. Here, we adopt the polar coordinate formulation, where the decision variables are voltage magnitude $V_{i,t} \in \left[V_{\min,i}, V_{\max,i}\right]$ and phase angle $\theta_{i,t} \in [-\pi, \pi]$ for each node $i \in I$ and time $t \in T$. The bus power balance is modeled, for all $i \in I$ and $t \in T$, by the non-convex equations

$$\sum_{g \in G_i} P^{\mathrm{G}}_{g,t} - P^{D}_{i,t} - V_{i,t} \sum_{k \in \mathcal{N}(i)} V_{k,t} \left(g_{ik} \cos\left(\theta_{i,t} - \theta_{k,t}\right) + b_{ik} \sin\left(\theta_{i,t} - \theta_{k,t}\right)\right) = 0, \tag{11}$$

$$\sum_{g \in G_i} Q^{\mathrm{G}}_{g,t} - Q^{D}_{i,t} - V_{i,t} \sum_{k \in \mathcal{N}(i)} V_{k,t} \left(g_{ik} \sin\left(\theta_{i,t} - \theta_{k,t}\right) - b_{ik} \cos\left(\theta_{i,t} - \theta_{k,t}\right)\right) = 0, \tag{12}$$

where g_{ik} and b_{ik} are given parameters characterizing the power grid. The complex voltage magnitude at each bus is constrained by the box bounds

$$V_{\min,i} \leq V_{i,t} \leq V_{\max,i}, \tag{13}$$

to ensure compliance with technical network specifications. The phase angle is naturally constrained within $-\pi \leq \theta_{i,t} \leq \pi$, with the reference node angle fixed as $\theta_{i,t} = \theta_{i,0}$, $\forall t \in T$. Furthermore, the transmission line capacity is constrained by the following inequalities, limiting current flow:

$$\left|\mathbb{I}_{l,t}\right|^2 \leq I^2_{\max,l}, \text{ for each } l \in L, \ t \in T. \tag{14}$$

Here, $\mathbb{I}_{l,t}$ denote the complex current through line l at time t, considering both 'from' and 'to' components of those magnitudes.

2.3 UC-ACOPF minimization problem

The UC-ACOPF is a non-convex MINLP which is formulated as follows:

$$
\text{[UC-AC]} \quad \begin{cases} \min\ (1) \\ \text{s.t.: } (2)-(14)\,, \\ \quad V_{i,t} \in \left[V_{\min,i}, V_{\max,i}\right],\ \theta_{i,t} \in [-\pi, \pi],\ i \in I, t \in T, \\ \quad \theta_{i,t} = \theta_{i,0},\ \forall t \in T, \quad \text{for the reference node}, \\ \quad Q^{\mathrm{G}}_{g,t} \in \left[Q_{\min,g}, Q_{\max,g}\right],\ \forall (g,t) \in G_{\mathrm{sc}} \times T, \\ \quad P^{\mathrm{G}}_{g,t} \in \{0\} \cup \left[P_{\min,g}, P_{\max,g}\right],\ \forall (g,t) \in G_{\mathrm{th}} \times T, \\ \quad Q^{\mathrm{G}}_{g,t} \in \{0\} \cup \left[Q_{\min,g}, Q_{\max,g}\right],\ \forall (g,t) \in G_{\mathrm{th}} \times T, \\ \quad P^{\mathrm{res}}_{g,t} \in \left[0, P_{\max,g} - P_{\min,g}\right],\ \forall (g,t) \in G_{\mathrm{th}} \times T, \\ \quad u_{g,t}, v_{g,t}, w_{g,t} \in \{0,1\},\ \forall (g,t) \in G_{\mathrm{th}} \times T. \end{cases}
$$

For clarity, we have assigned labels to certain problems discussed in this paper; thus, we will refer to the previous problem as problem [UC-AC] or simply [UC-AC], and we will use the same criteria for other labeled problems. A point $(\boldsymbol{x}, \boldsymbol{y})$ is considered UC-feasible if satisfies constraints (2)-(4) and (7)-(8) and AC-feasible if it satisfies constraints (11)-(14). For simplicity, reserve requirements and other minor constraints are omitted in this classification. A point is considered feasible for UC-ACOPF if it satisfies all the constraints in problem [UC-AC].

3 Relax-and-round strategies

In this paper, we propose different heuristic approaches to efficiently obtain feasible points for the UC-ACOPF problem using relax-and-round strategies. These methods relax integer constraints, solve the resulting continuous optimization problem, and then round the solution to restore feasibility while preserving near-optimality.

The Relaxed Unit Commitment (RUC) problem is a linear programming (LP) relaxation of the UC problem, where the binary variables $u_{i,t}$, $v_{i,t}$ and $w_{i,t}$ are allowed to take values in [0, 1]. Since constraints (2)-(4) enforce the binary logic on $v_{g,t}$ and $w_{g,t}$ whenever $u_{i,t}$ is binary, the discussion of the integer relaxation of the problem focuses primarily on the decision variables $u_{g,t}$. Extending this relaxation to the UC-ACOPF formulation leads to the RUC-ACOPF problem, a non-convex nonlinear programming (NLP) problem, where the integrality constraints on $u_{g,t}$, $v_{g,t}$ and $w_{g,t}$ is relaxed as follows:

$$
\text{[RUC-AC]} \quad \begin{cases} \min\ (1) \\ \text{s.t.: } (2)-(14), \\ \quad \tilde{V}_{i,t} \in \left[V_{\min,i}, V_{\max,i}\right],\ \tilde{\theta}_{i,t} \in [-\pi, \pi],\ i \in I, t \in T, \\ \quad \tilde{\theta}_{i,t} = \tilde{\theta}_{i,0},\ \forall t \in T, \quad \text{for the reference node}, \\ \quad \tilde{Q}^{\mathrm{G}}_{g,t} \in \left[Q_{\min,g}, Q_{\max,g}\right],\ \forall (g,t) \in G_{\mathrm{sc}} \times T, \\ \quad \tilde{P}^{\mathrm{G}}_{g,t} \in \left[0, P_{\max,g}\right],\ \forall (g,t) \in G_{\mathrm{th}} \times T, \\ \quad \tilde{Q}^{\mathrm{G}}_{g,t} \in \left[\min\{Q_{\min,g}, 0\}, \max\{Q_{\max,g}, 0\}\right],\ \forall (g,t) \in G_{\mathrm{th}} \times T, \\ \quad \tilde{P}^{\mathrm{res}}_{g,t} \in \left[0, P_{\max,g} - P_{\min,g}\right],\ \forall (g,t) \in G_{\mathrm{th}} \times T, \\ \quad \tilde{u}_{g,t}, \tilde{v}_{g,t}, \tilde{w}_{g,t} \in [0,1],\ \forall (g,t) \in G_{\mathrm{th}} \times T. \end{cases}
$$

To distinguish the decision variables in [RUC-AC] from their counterpart in [UC-AC] we use a tilde notation. The relax-and-round strategy begins by relaxing the integrality condition on the binary variables in [UC-AC] to obtain [RUC-AC]. Fixing $u_{g,t}, v_{g,t}, w_{g,t}$ in [UC-AC] results in a non-convex NLP problem here referred to as the ACOPF problem or problem [ACOPF]. After solving [RUC-AC], the relaxed variables $\tilde{u}_{g,t}, \tilde{v}_{g,t}, \tilde{w}_{g,t}$ are rounded *somehow* to binary values. These values are then fixed in [UC-AC] to obtain [ACOPF], which is finally solved to determine feasible values for the remaining decision variables.

The key advantage of this strategy is that solving the relaxed problem [RUC-AC], which is a non-convex NLP problem, should be conceptually simpler and significantly faster than solving the original [UC-AC], a non-convex MINLP problem. However, the rounded binary solution from [RUC-AC] is often unsuitable point for the UC-ACOPF problem due to two main issues. First, the relaxation eliminates the combinatorial nature of the mixed-integer constraints, meaning that simple rounding may not ensure UC feasibility. Second, relaxing $u_{g,t} \in \{0,1\}$ to $\tilde{u}_{g,t} \in [0,1]$, transforms the domain of $P^{\mathrm{G}}_{g,t}$ from a disconnected set $\{0\} \cup [P_{\min,g}, P_{\max,g}]$ into a continuous one $\tilde{P}^{\mathrm{G}}_{g,t} \in \left[0, P_{\max,g}\right]$, altering the behavior of the active power transitions. To avoid this, and before rounding, we introduce a transformation that converts $\tilde{u}_{g,t}$ into a more 'roundable' variable $\tilde{u}^{r}_{g,t}$, as explained in the next section. Additionally, we propose an enhanced rounding formula to ensure the feasibility of constraints (2)-(4) and better enforce UC-feasibility. However, general feasibility or optimality are not guaranteed; in this sense, we sometimes abuse the notation by referring to the points returned by the algorithms as 'solutions'.

3.1 Making the relaxed solution 'roundable'

As previously discussed, relaxing $u_{g,t}$ to $[0,1]$ changes the properties of the UC-ACOPF problem. In the original problem, $P^{\mathrm{G}}_{g,t}$ must be either zero or at least $P_{\min,g}$, whereas in the relaxed problem [RUC-AC], thermal units can inject only the minimum amount of power needed to satisfy the demand within the range $\left[0, P_{\max,g}\right]$. Furthermore, while the costs associated with the binary variables $u_{g,t}$, $v_{g,t}$ and $w_{g,t}$ are constant in (1), their relaxed counterparts $\tilde{u}_{g,t}, \tilde{v}_{g,t}, \tilde{w}_{g,t} \in [0,1]$ exhibit linearly

increasing costs. Consequently, when solving [RUC-AC], these variables will only approach 1 if required for feasibility or if it is more cost-effective than remaining near zero. The main reason for $\tilde{u}_{g,t}$ tending towards 1 is to allow $\tilde{P}^{\mathrm{G}}_{g,t}$ to approach $P_{\max,g}$, since

$$P_{\min,g}\tilde{u}_{g,t} \leq \tilde{P}^{\mathrm{G}}_{g,t} \leq P_{\max,g}\tilde{u}_{g,t}, \tag{15}$$

assuming $P^{\mathrm{res}}_{g,t} = 0$. Thus, $\tilde{u}_{g,t}$ does not directly represent the binary on/off status of the unit. Instead, $\tilde{u}_{g,t} = 1$ indicates that the plant operates at maximum capacity, but the actual commitment status remains undefined due to the relaxation.

The previous reasons intuitively justify why [RUC-AC] solutions can deviate from the solutions to problem [UC-AC]. However, if a direct rounding approach is to be used, we wondered if it might be interesting to redefine *which quantity* from the relaxed solution should be rounded. If we assume that the main role of $\tilde{u}_{g,t}$ is to allow $\tilde{P}_{g,t}$ to reach a power level $\tilde{u}_{g,t}P_{\max,g}$, and that the relaxed problem retains useful information from the relaxed combinatorial relationships of the original [UC-AC], then we can set

$$\tilde{u}_{\min,g} = \frac{P_{\min,g}}{P_{\max,g}}, \tag{16}$$

as a minimum reference for $\tilde{u}_{g,t}$, modeling the on/off status of the power plant $g \in G_{\mathrm{th}}$, $\forall t \in T$. If $\tilde{P}^{\mathrm{G}}_{g,t} \geq P_{\min,g}$ it is reasonable to expect $u_{g,t} = 1$ in a solution for [UC-AC]. For this to happen, taking into account (15), necessarily $\tilde{u}_{g,t} \geq P_{min,g}/P_{\max,g}$. Then, if $\tilde{u}_{g,t} \geq \tilde{u}_{\min,g}$, we should round $\tilde{u}_{g,t}$ to 1 when fixing $u_{g,t}$. Although the value (16) varies for each thermal power plant, it has the same meaning for all of them; this homogenizes the criteria for rounding since the parameters characterizing each $g \in G_{\mathrm{th}}$ affect the behavior of $\tilde{u}_{g,t}$ through the relaxed version of the mixed-integer constraints.

Based on this idea, we introduce two strategies to modify $\tilde{u}_{g,t}$ into $\tilde{u}^r_{g,t}$, producing values better suited for direct rounding. The first strategy, Re-RUC, rescales $\tilde{u}_{g,t}$ by the inverse of $\tilde{u}_{\min,g}$, yielding

$$\text{(Re-RUC)} \quad \tilde{u}^r_{g,t} = \frac{1}{\tilde{u}_{\min,g}}\tilde{u}_{g,t} = \frac{P_{\max,g}}{P_{\min,g}}\tilde{u}_{g,t}.$$

The second strategy, Re-Power, rescales $\tilde{P}_{g,t}$ and defines the rounding variable as

$$\text{(Re-Power)} \quad \tilde{u}^r_{g,t} = \frac{\tilde{P}_{g,t}}{P_{\min,g}}.$$

This second approach has been used previously in rounding-based methods. For example, in He et al. (2016), to get an initial integer solution for a feasibility pump algorithm. Also in Wang et al. (2021), combined with what we later refer to 'naive rounding formula', rounding values around a fixed threshold. Since each relaxed value is rescaled using parameters specific to its corresponding power plant, strategies (Re-RUC) and (Re-Power) are not equivalent to uniformly rescaling all values unless all power plants share the same parameters.

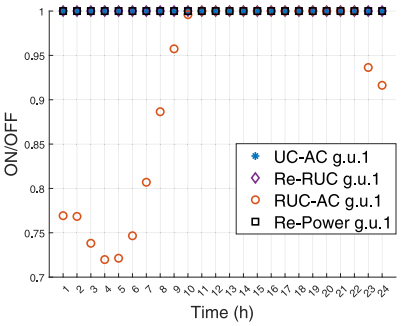

(a) Generation unit 1.

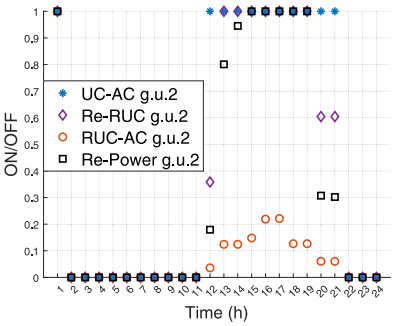

(b) Generation unit 2.

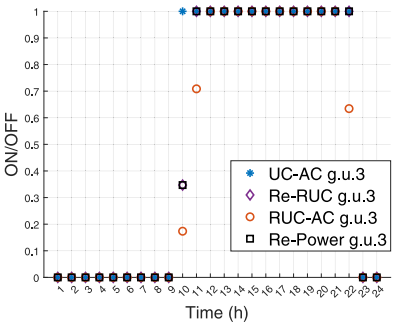

(c) Generation unit 3.

Fig. 1 On/off status of the 3 power plants in the 6-bus test system example.

In this work, the goal is to numerically evaluate the performance of these strategies by comparing them to the standard approach:

$$\tilde{u}^r_{g,t} = \tilde{u}_{g,t}. \tag{17}$$

The numerical experiments will be detailed in the following sections. However, to illustrate the main features of these strategies at this stage, we present some preliminary rescaling results. Figure 1 shows an example for the 6-bus test system Fu et al. (2006), comparing the integer solution $u_{g,t}$, the relaxed solution $\tilde{u}_{g,t}$ obtained using a local NLP solver, and the two proposed rescaling strategies, Re-RUC and Re-Power. After rescaling, some values of $\tilde{u}^r_{g,t}$ may exceed 1. In Fig. 1, these values are rounded down to 1 before plotting. For relaxed values within (0, 1), the proposed approaches are expected to make it easier to recover the 'desired' integer solution using the natural rounding formula around 0.5. As we will see later, this property can improve the feasibility rate of solutions returned relax-and-round heuristics, particularly direct rounding formulas, which we discuss next.

3.2 Rounding formulas

In this section we first discuss the standard or naive rounding (NR) formula, which assigns values above 0.5 to 1 and those at or below 0.5 to 0. This simple approach often leads to infeasible UC solutions. To overcome its limitations, we introduce heuristic refinements that form the Enhanced Rounding (ER) formula, which provides a more systematic rounding procedure but still lacks guarantees of AC-feasibility. UC feasibility is not ensured either, primarily because combinatorial constraints involving minimum up/down times, T_g^u and T_g^d, are not fully considered. To address this, we propose the UC Enhanced Rounding UC-ER formula, outlined in Algorithm 1. This heuristic rounding strategy is applied sequentially over the discrete time steps. At each time step the decisions made in earlier steps are taken into account, thereby incorporating the plant's operational constraints; nevertheless, past unit commitment decisions cannot be modified.

As illustrated in Fig. 1, NR may fail to recover the correct integer solution because, in practice, rounding is performed without prior knowledge of which integer solution should be targeted. For example, applying NR to the relaxed solution $\tilde{u}_{g,t}$ (red circle), could incorrectly round values below 0.5 to zero, turning off units that we would like to remain committed, comparing them with the desired integer solution of reference. Although our rescaling strategies, (Re-RUC) and (Re-Power), produce a more 'roundable' relaxed solution $\tilde{u}^r_{g,t}$, some problematic cases persist (e.g., unit 2 at times 12, 20, and 21, and unit 3 at time 10). In response to such problems, some authors suggest the use of thresholds closer to or equal to zero to avoid committing units that cannot effectively meet the energy demand Kjeldsen and Chiarandini (2012), Sawa et al. (2007). One possible strategy is progressive rounding, which sorts relaxed values in descending order and rounds them in groups (e.g., [0.9, 1), [0.8, 0.9), etc.), ensuring that higher values are processed first to improve feasibility. In Algorithm 1, we prioritize rounding by grouping $\tilde{u}^r_{g,t}$ into descending intervals, referred to as rounding levels, whose size can be adjusted to approximate strict descending order, making the implementation more flexible. However, when using this approach, a stopping criterion is essential to avoid over-committing generation units. Here, over-committing refers to propose feasible points with an unnecessarily large number of committed units, compared to a more cost-optimal solution for the same instance. A natural criterion could be to stop rounding at each time when the total power generation equals the total demand, namely,

$$P_t^D := \sum_{i \in I_D} P_{i,t}^D. \tag{18}$$

We decided to track the amount of power committed after each rounding decision. When $\tilde{u}^r_{g,t}$ is rounded so that $u_{g,t} = 1$, thermal generating unit $g \in G_{\text{th}}$ is committed, and its relaxed power generation $\tilde{P}^{\text{G}}_{g,t}$ is added to the total committed power P_t^{G}. In other words, the contribution of committed plants at each time step is tracked by adding their power generation from the relaxed solution. This total is then compared with the system demand to ensure sufficient power has been committed, by verifying that $P_t^{\text{G}} \geq P_t^D$. At each time step, if the dispatched power meets or exceeds the demand, no further unit commitment is necessary, and the remaining $\tilde{u}^r_{g,t}$ are rounded

to zero. The algorithm would then proceed to the next time step. This stop condition is implemented in line 15 of Algorithm 1.

Notice that if we apply the Re-Power rescaling (Re-Power), $\tilde{u}^r_{g,t} \geq 1$ ensures that the power generation $\tilde{P}^{\mathrm{G}}_{g,t}$ is at least equal to the minimum required power $P_{\min,g}$ for unit g, thereby guaranteeing that the unit meets its minimum generation requirement. However, for the Re-RUC strategy (Re-RUC), this is not necessarily true, as $\tilde{u}_{g,t}$ are involved in additional constraints. Nevertheless, as we rely on a relax-and-round strategy, and any direct heuristic decision outside an optimization framework may introduce uncompensated biases, we choose to automatically commit units whenever $\tilde{u}^r_{g,t} \geq 1$. In order to incorporate the minimum up- and down-time constraints, lines 4-11 first address the plants that must be mandatorily committed. Then, in line 13 the remaining plants are grouped according to the relaxed solution, with those satisfying $\tilde{u}^r_{g,t} \geq 1$ being the first ones to which the decision criteria, explained next, are applied in line 18.

First, if the unit is committed, it must generate at least its minimum power output, $P_{\min,g}$, according to the constraints of the UC-ACOPF problem. In such a case, rather than simply adding $\tilde{P}^{\mathrm{G}}_{g,t}$ to the total committed power P^{G}_t, we should add the greater of $\tilde{P}^{\mathrm{G}}_{g,t}$ and $P_{\min,g}$, ensuring that the unit generates enough power to remain within the feasible region:

$$P^{\mathrm{G}}_t \leftarrow P^{\mathrm{G}}_t + \max\{\tilde{P}^{\mathrm{G}}_{g,t}, P_{\min,g}\}.$$

If $P_{\min,g} > \tilde{P}^{\mathrm{G}}_{g,t}$, we must also ensure that the additional power, $P_{\min,g} - \tilde{P}^{\mathrm{G}}_{g,t}$, is tracked to avoid overgeneration.

Then, we want to check whether it is possible to reduce the committed power elsewhere in the system to balance the excess power generated by units operating at their minimum levels. To achieve this, we define a slack power, $P^{\mathrm{G}}_{\mathrm{s},t}$, which initially represents the total power generated above $P_{\min,g}$. When committing a generating unit, the slack power should be updated, for example, by adding $-P_{\min,g} + \tilde{P}^{\mathrm{G}}_{g,t}$ (which could be negative). However, to be more accurate, we must account for ramping limits that constrain how much a generating unit's output can change between time steps. Thus, we update the slack power tracker as:

$$P^{\mathrm{G}}_{\mathrm{s},t} \leftarrow P^{\mathrm{G}}_{\mathrm{s},t} + \min\{R^d_g - \tilde{P}^{\mathrm{G}}_{g,t-1} + \tilde{P}^{\mathrm{G}}_{g,t}, -P_{\min,g} + \tilde{P}^{\mathrm{G}}_{g,t}\}.$$

Finally, we can track the potential power generation, $P^{\mathrm{G}}_{\mathrm{p},t}$, based on the commitment decisions made up to any point in the rounding process. This quantity can be used to ensure that reserve requirements are met. Assuming a single region for power demand constraints, the condition

$$\sum_{g \in G_{\mathrm{th}}} \tilde{P}^{\mathrm{res}}_{g,t} u_{g,t} + P^{\mathrm{G}}_{\mathrm{p},t} > P^{\mathrm{res}}_{r,t}$$

can be used as an additional stopping criterion during the rounding process. After deciding for all $g \in G_{\mathrm{th}}$, $P^{\mathrm{G}}_{\mathrm{p},t}$ can also be used to verify whether the demand can be

Algorithm 1 UC Enhanced Rounding UC-ER formula

Require: Relaxed and rescaled solution $\tilde{u}^r_{g,t}$, global power demand for each time P^D_t, an array of rounding levels $lvl\,(\cdot)$ in [0, 1] of size N_{lvl} and some grid data.

Initialize $u_{g,t} \leftarrow 0$ for all g and t.
for $t \leftarrow 1$ **to** t_f **do**
  Initialize $P^{\mathrm{G}}_t \leftarrow 0$, $P^{\mathrm{G}}_{\mathrm{p},t} \leftarrow 0$, $P^{\mathrm{G}}_{\mathrm{s},t} \leftarrow 0$.
  Classify the power plants as forced Cg or free FCg to commit.
  for $g \in Cg$ **do**
    $u_{g,t} \leftarrow 1$,
    $P_{\mathrm{s,a}} \leftarrow P_{\min,g} - \tilde{P}^{\mathrm{G}}_{g,t}$,
    $\tilde{P}^{\mathrm{G}}_{g,t} \leftarrow \max\{P_{\min,g}, \tilde{P}^{\mathrm{G}}_{g,t}\}$,
    $P^{\mathrm{G}}_t \leftarrow P^{\mathrm{G}}_t + \tilde{P}^{\mathrm{G}}_{g,t}$,
    $P^{\mathrm{G}}_{\mathrm{p},t} \leftarrow P^{\mathrm{G}}_{\mathrm{p},t} + u_{g,t-1}\left(R^u_g - \tilde{P}^{\mathrm{G}}_{g,t} - \tilde{P}^{\mathrm{res}}_{g,t} + \tilde{P}^{\mathrm{G}}_{g,t-1}\right) + \left(1 - u_{g,t-1}\right)\left(S^u_g - \tilde{P}^{\mathrm{G}}_{g,t} - \tilde{P}^{\mathrm{res}}_{g,t}\right)$,
    $P^{\mathrm{G}}_{\mathrm{s},t} \leftarrow P^{\mathrm{G}}_{\mathrm{s},t} + \min\{R^d_g - \tilde{P}^{\mathrm{G}}_{g,t-1} + \tilde{P}^{\mathrm{G}}_{g,t}, P_{\mathrm{s,a}}\}$.
  end for
  Classify FCg by rounding levels given by $lvl\,(\cdot)$.
  for $l \leftarrow N_{lvl}$ **to** 1 **do**
    If $P^{\mathrm{G}}_t > P^D_t$ and $\sum_{g \in G_t} \tilde{P}^{\mathrm{res}}_{g,t} u_{g,t} + P^{\mathrm{G}}_{\mathrm{p},t} \geq P^{\mathrm{res}}_{r,t}$ **then** $t + 1$ **and go to** 3:
    for $g \in lvl\,(l)$ **do**
      $dP \leftarrow P_{\min,g} - P_{g,t}$,
      if $\left(P^{\mathrm{G}}_{\mathrm{s},t} > dP\right)$ and $\left(P^{\mathrm{G}}_t + P_{\min,g} - (P^{\mathrm{G}}_{\mathrm{s},t} - dP) < PD(t)\right)$ **then**
        $u_{g,t} \leftarrow 1$,
        $P_{\mathrm{s,a}} \leftarrow P_{\min,g} - \tilde{P}^{\mathrm{G}}_{g,t}$,
        $\tilde{P}^{\mathrm{G}}_{g,t} \leftarrow \max\{P_{\min,g}, \tilde{P}_{g,t}\}$,
        $P^{\mathrm{G}}_t \leftarrow P^{\mathrm{G}}_t + \tilde{P}^{\mathrm{G}}_{g,t}$,
        $P^{\mathrm{G}}_{\mathrm{p},t} \leftarrow P^{\mathrm{G}}_{\mathrm{p},t} + u_{g,t-1}\left(R^u_g - \tilde{P}^{\mathrm{G}}_{g,t} - \tilde{P}^{\mathrm{res}}_{g,t} + \tilde{P}^{\mathrm{G}}_{g,t-1}\right)$
          $+ \left(1 - u_{g,t-1}\right)\left(S^u_g - \tilde{P}^{\mathrm{G}}_{g,t} - \tilde{P}^{\mathrm{res}}_{g,t}\right)$,
        $P^{\mathrm{G}}_{\mathrm{s},t} \leftarrow P^{\mathrm{G}}_{\mathrm{s},t} + \min\{R^d_g - \tilde{P}^{\mathrm{G}}_{g,t-1} + \tilde{P}^{\mathrm{G}}_{g,t}, P_{\mathrm{s,a}}\}$.
      end if
    end for
  end for
end for

met, i.e., if $P^{\mathrm{G}}_{\mathrm{p},t} + P^{\mathrm{G}}_t > P^D_t$. If this condition is not satisfied, it indicates that the rounding procedure may have failed for that time step.

Once the commitment decisions from the UC-ER formula are fixed and the ACOPF problem is solved, the full set of UC-skeleton and other constraints will be enforced, and we hope for a feasible point for the UC-ACOPF problem to be returned.

3.3 Relax-and-round algorithm

We now formalize our proposed direct approach, leveling on the relaxation and rounding formulas discussed in the previous sections. The main steps of the methodology are summarized in Algorithm 2. In step 3, one can choose between: the standard approach (17), the rescaling for $\tilde{u}_{g,t}$ (Re-RUC) or the rescaling based on $\tilde{P}^{\mathrm{G}}_{g,t}$ (Re-Power). In step 4, the NR, ER, or UC-ER formulas can be applied. In general, any other appropriate rounding approach can be used.

Algorithm 2 Relax-and-round with formulas

1: Consider an instance of problem [UC-AC].
2: Solve [RUC-AC] obtaining $\tilde{u}_{g,t}$.
3: Rescale $\tilde{u}_{g,t}$ to obtain $\tilde{u}^r_{g,t}$.
4: Round $\tilde{u}^r_{g,t}$ using a rounding formula. Let $\boldsymbol{y}_{\mathrm{R}}$ be then the integer solution.
5: Fix the integer variables $\boldsymbol{y} = \boldsymbol{y}_{\mathrm{R}}$ in [UC-AC], obtaining [ACOPF]. Solve [ACOPF]. Let $\boldsymbol{x}_{\mathrm{AC}}$ be its solution.
6: Return $\left(\boldsymbol{x}_{\mathrm{AC}}, \boldsymbol{y}_{\mathrm{R}}\right)$.

4 Numerical results of the direct relax-and-round strategies

This section presents numerical results for the UC-ACOPF problem, applying the direct relax-and-round approach to two benchmark test systems: the 6-bus test system and a modified IEEE 118-bus system. The goal is to assess the feasibility of the solutions obtained using the proposed rescaling strategies and rounding formulas. Nevertheless, we also report results for these benchmark systems obtained with established operational baselines, including the classic UC formulation without network constraints and the UC problem with DC power flow equations (UC-DCOPF), as well as UC-ACOPF solutions reported in the literature. Here, UC-DCOPF refers to the unit commitment problem in which network constraints are modeled using the DC power flow approximation. This is a linear approximation obtained from the AC power flow equations by assuming negligible line resistance compared to line reactances, fixed voltage magnitudes (typically 1 p.u.), and small phase-angle differences across transmission lines (see Anjos et al. (2017)). Because globally solving UC-ACOPF is computationally demanding in unit commitment applications, UC-DCOPF remains a widely used tractable reference in operations and in the literature. Accordingly, we report UC-DCOPF benchmarks from Castillo et al. (2016) only as a baseline to provide context for our AC-feasible UC-ACOPF results.

To solve the [RUC-AC] and [ACOPF] problems, we use classical penalized sequential linear programming (PSLP) algorithms, following the parameter notation in Bazaraa et al. (2006). PSLP linearizes nonlinear constraints and the cost function via first-order Taylor expansion. Slack variables are incorporated into the linearized constraints to ensure feasibility and are penalized in the cost function.

The initial guess for the decision variables in step 2 of Algorithm 2 is a modified flat value for the complex voltage and the generation commitment at t_0 for the power plants across the 24-hour horizon. In particular, we set $V_{i,t} = \left(V_{\max,i} + V_{\min,i}\right)/2$, for all $t \in T$. This prevents the initial guess, at the start of the PSLP algorithm, from lying outside or exactly on its upper or lower bounds when the voltage is directly fixed at 1 in the per-unit (p.u.) system. In step 5, the algorithm PSLP algorithm is also initialized with a modified flat voltage profile, while power generation commitments are set according to the rounded binary values.

Once these commitments are fixed, initial values are assigned to the active and reactive power. For example, the reactive power $Q^{\mathrm{G}}_{t,g}$ is set to 0 for all power plants, and active power $P^{\mathrm{G}}_{t,g}$ is set close to the plant's minimum operating level $P_{\min,g}$ when the plant is committed (i.e., $u_{g,t} = 1$) or 0 if the plant is not committed (i.e., $u_{g,t} = 0$). This ensures the basic UC constraints are satisfied. Although this setup may

Table 1 Values of the parameters for the PSLP algorithms.

Stop ϵ	Penalty	ρ_0	ρ_1	ρ_2	β	Δ_{LB}
1e−4	5e6	1e−6	0.25	0.75	0.5	1e−6

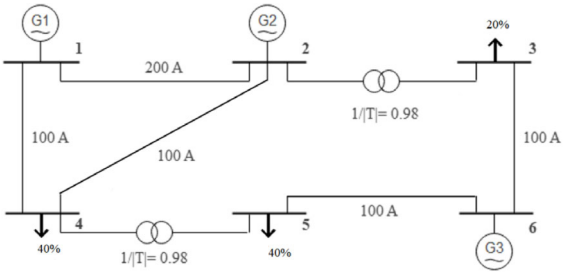

Fig. 2 6-bus test system circuit.

be AC infeasible, the PSLP algorithm can still proceed because it introduces penalized slack variables that allow flexibility in satisfying the linearized AC constraints during iterations.

The PSLP method is a local minimizer, with several parameters involved that affect both the performance and solutions quality. The selected parameter values are detailed in Table 1. Additionally, in step 2, we tested different penalty weights {5.e3, 5.e4, 5.e5, 5.e6, 5.e7} to solve the problem [RUC-AC], leading to variations in $\tilde{u}_{g,t}$ and, consequently, different integer solutions after rounding. These values were selected empirically based on numerical experiments.

The main program implementing the different algorithms presented in this paper is written in Fortran. Also, all the linear problems involved are solved using Gurobi v9.5.2 Gurobi Optimization (2023). The feasibility of the solutions is double-checked with SCIP Achterberg (Jul 2009) via NEOS Server Czyzyk et al. (1998) or MAinGO Najman et al. (2019). The default configuration is used for all solvers. The feasibility tolerance is set to 1e−6 and the PSLP parameters are chosen accordingly. A solution is considered (numerically) AC-feasible if the constraints (11)-(14) hold within this tolerance. As is standard practice, the ACPF equations are normalized using the per-unit system.

4.1 6-bus test system

The first example is the 6-bus test system from Fu et al. (2005), modeled as shown in Fig. 2. It consists of 6 buses and 7 elements: 2 tap-changing transformers and 5 transmission lines. There are 3 thermal generators placed on buses 1, 2, and 6, and loads or power demands on buses 3, 4, and 5. Despite its small size, (216 binary and 1344 continuous variables), global solvers available in NEOS and MAiNGO fail to solve it within 8 hours using their standard configurations.

Table 2 summarizes the performance of our direct strategy, using different rescaling and rounding combinations. In Table 2, and in the subsequent tables reporting comparable results, columns 1st and 2nd PSLP denote the application of the PSLP algorithm to [RUC-AC] and [ACOPF] problems, respectively. The AC-feas column

reports the feasibility tolerance of the point returned by the PSLP with respect to the ACPF equations (for the 2nd PSLP, this corresponds to the final point of Algorithm 2). Furthermore, the Feas. column indicates the overall feasibility of that point for the UC-ACOPF problem, considering all of its constraints: the green check marks indicate UC-ACOPF feasible points, while the red crosses correspond to infeasible ones.

Results are shown for a penalty weight of 5e6 in the 1st PSLP used for solving problem [RUC-AC], as similar outcomes were observed for other values. In particular, the NR formula failed to produce a feasible solution within the specified tolerance of 1e−6, though the Re-RUC approach showed better feasibility than the other two methods. For the ER and UC-ER rounding strategies, the rescaling approach had no significant impact, as both consistently produced the same feasible UC-ACOPF solution.

Table 3 reports the commitment schedule recovered by the UC-ER formula and compares it with schedules available in the literature for the same test system, including an equivalent UC-ACOPF formulation, a classical UC model, and a UC-DCOPF formulation. The resulting commitments and the corresponding AC operating costs are consistent with the global solution reported in Liu et al. (2018) and comparable to those obtained with a local solver in Castillo et al. (2016), allowing a direct comparison between the UC solution and the relaxed RUC solution. In this case, the binary variables and their relaxed counterparts are directly linked through the UC-ER and ER rounding formulas, ensuring that applying these formulas to the relaxed solutions consistently yields the same integer commitment. For a detailed comparison of the resulting power system operating points across the different formulations, we refer the reader to Castillo et al. (2016).

The effects of the relaxation on the binary variables for the 6-bus test system were previously illustrated in Fig. 1. Since problems [RUC-AC] and [UC-AC] are non-convex, direct comparisons of their AC state solutions are generally not very informative due to the presence of multiple local optima. The relaxed problem, [RUC-AC], produces smoother time profiles because relaxing the integer constraints eliminates abrupt jumps in the generator on/off states, thereby reducing time coupling effects. Consequently, while UC-ACOPF solutions exhibit sudden changes in generation and power flow, RUC-ACOPF allows for more gradual transitions.

Figures 3 and 4 compares total active and reactive power generation for both solutions. While their profiles are similar, the relaxed solution does not enforce minimum generation constraints as in the integer-constrained problem. Instead, RUC-ACOPF allows units to generate below their minimum output, prioritizing cheaper units (in ascending cost order: g.u. 1, 3, and 2, assuming power plant 1 is already on). Higher-cost units are committed only when necessary, leading to a different distribution of active power across units. Figure 4 shows a significant discrepancy in reactive power generation, which affects the power balance in the grid and leads to qualitative and quantitative differences in bus voltages, and power flow in the lines. These differences explain the challenges in achieving AC feasibility when solving problem [ACOPF] after rounding the relaxed unit commitment.

Table 2 Summary of the direct approaches performance for the 6-bus test system example.

			1st PSLP		2nd PSLP			Results	
Rescale	**Round**	Penalty	Iter.	AC-feas.	Iter.	AC-feas.	Feas.	Cost($)	Time (s)
None	Naive	5e6	5	3.16e−13	17	4.12e1	✗	94704	2.7
Re-RUC	Naive	5e6	5	3.16e−13	32	6.17e−2	✗	101058	3.8
Re-Power	Naive	5e6	5	3.16e−13	30	7.53e1	✗	100230	3.6
None	ER	5e6	5	3.16e−13	34	1.86e−8	✓	101763	4.0
Re-RUC	ER	5e6	5	3.16e−13	34	1.86e−8	✓	101763	4.0
Re-Power	ER	5e6	5	3.16e−13	34	1.86e−8	✓	101763	3.9
None	UC-ER	5e6	5	3.16e−13	34	1.86e−8	✓	101763	4.0
Re-RUC	UC-ER	5e6	5	3.16e−13	34	1.86e−8	✓	101763	4.0
Re-Power	UC-ER	5e6	5	3.16e−13	34	1.86e−8	✓	101763	4.0

Table 3 Comparison between commitment and cost solutions for the 6-bus test system example.

	Castillo et al. (2016)		Liu et al. (2018)	Rescale + Round strategy	
	UC	UC-DCOPF	UC-ACOPF	Re-Power+UC-ER(*)	Re-RUC+NR
Cost($)	101269	106887	101763	101763 ✓	101058 ✗
g.u. 1	1-24	1-24	1-24	1-24	1-24
g.u. 2	1,12-21	1,11-22	1,12-21	1,12-21	1,13-21
g.u. 3	10-22	10-22	10-22	10-22	11-22

(*) Also, all combinations including the different rescale and the ER and UC-ER formulas

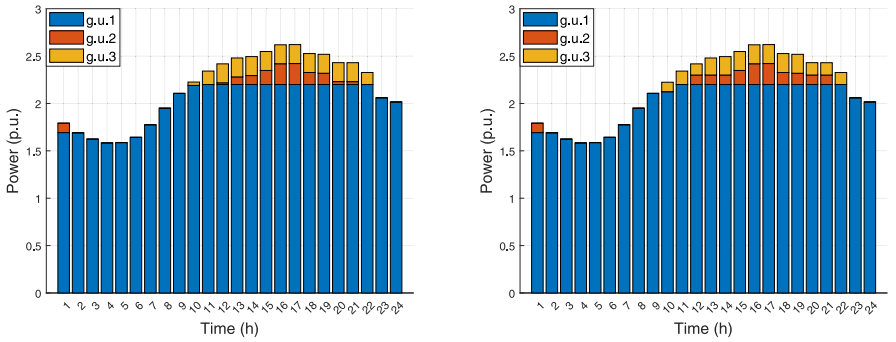

(a) [RUC-AC] (b) [UC-AC]

Fig. 3 Active power generation in the 6-bus test system example.

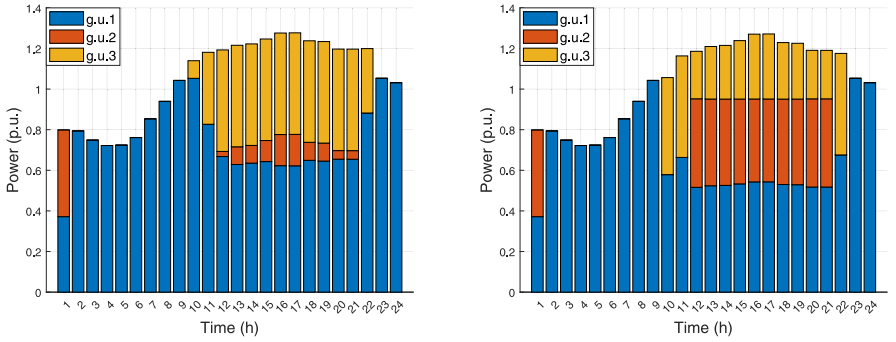

(a) [RUC-AC] (b) [UC-AC]

Fig. 4 Reactive power generation in the 6-bus test system example.

4.2 118-bus test system

This section presents numerical results for the modified IEEE 118-bus test system from Castillo et al. (2016). It consists of 118 buses, 54 thermal generators, 14 synchronous condensers, and 186 elements: 8 tap-changing transformers, 1 phase shifter, and 177 transmission lines. This medium-size benchmark is widely used to evaluate the scalability of solvers for the UC-ACOPF problem. No MINLP solver available on

Table 4 Summary of the NR formula performance for the 118-bus test system example.

Naive Round (NR)								
		1st PSLP		2nd PSLP		Results		
Rescale	Penalty	Iter.	AC-feas.	Iter.	AC-feas.	Feas.	Cost($)	Time (s)
None	5e3	276	9.13e−6	123	1.24e+1	✗	740619	993
Re-RUC	5e3	276	9.13e−6	40	2.71e−8	✓	847460	850
Re-Power	5e3	276	9.13e−6	41	2.61e−8	✓	846272	852
None	5e4	40	5.51e−6	351	1.07e+1	✗	741383	717
Re-RUC	5e4	40	5.51e−6	41	2.65e−8	✓	847633	197
Re-Power	5e4	40	5.51e−6	41	2.65e−8	✗	846332	192
None	5e5	36	1.10e−6	370	1.01e+1	✗	760409	761
Re-RUC	5e5	36	1.10e−6	39	2.64e−8	✓	847742	179
Re-Power	5e5	36	1.10e−6	41	2.61e−8	✗	846432	184
None	5e6	39	2.46e−8	184	1.02e+1	✗	759607	438
Re-RUC	5e6	39	2.46e−8	40	2.77e−8	✓	847740	191
Re-Power	5e6	39	2.46e−8	41	2.58e−8	✓	846543	194
None	5e7	44	3.45e−9	228	9.97	✗	740015	529
Re-RUC	5e7	44	3.45e−9	41	2.56e−8	✓	847713	209
Re-Power	5e7	44	3.45e−9	41	2.67e−8	✗	846527	211

the NEOS server was able to return a solution after 8 hours of computation for this test using their standard configurations, which is consistent with the results reported in Tejada-Arango et al. (2019b). We first analyze results where descending and rounding procedures have been applied to $\tilde{u}^r_{g,t}$ based on strict value ordering. In addition, results are given for all the penalty weight values listed at the beginning of the section 4.

Table 4 summarizes the performance of the NR formula, highlighting the impact of rescaling on feasibility. Without rescaling $\tilde{u}^r_{g,t}$, no feasible solution was found. The Re-RUC approach consistently produced UC-feasible integer solutions, achieving AC feasibility in step 5 of Algorithm 2. Conversely, the Re-Power approach only achieved feasible points for some of the considered penalty weights. Additionally, Re-Power resulted in lower solution costs compared to Re-RUC. In summary, Re-RUC rescaling proves to be the most reliable rescaling method for the NR formula in terms of consistently producing feasible solutions. By contrast, for the ER formula, all solutions were AC-feasible but none were UC-feasible, which is consistent with its design. Since Re-RUC successfully recovered UC-feasible solutions when applied to NR, this outcome suggests that the ER formula may overwrite useful information contained in the relaxed and rescaled solution.

Table 5 summarizes the results for the UC-ER formula. All solutions obtained were feasible. While rescaling did not affect feasibility, the Re-Power method consistently produced the lowest cost feasible solution.

Next, we set the 1st PSLP penalty weight in step 2 to 5e6 and repeated the experiments, this time grouping $\tilde{u}^r_{g,t}$ values into different intervals, with each subsequent experiment increasing the interval size. Generators within each interval were ordered

Table 5 Summary of the UC-ER formula performance for the 118-bus test system example.

UC Enhanced Round (UC-ER)								
		1st PSLP		2nd PSLP		Results		
Rescale	Penalty	Iter.	AC-feas.	Iter.	AC-feas.	Feas.	Cost($)	Time (s)
None	5e3	276	9.13e−6	42	2.52e−8	✓	850421	833
Re-RUC	5e3	276	9.13e−6	40	2.6e−8	✓	851634	835
Re-Power	5e3	276	9.13e−6	41	2.54e−8	✓	849031	837
None	5e4	40	5.51e−6	38	2.48e−8	✓	851200	187
Re-RUC	5e4	40	5.51e−6	40	2.54e−8	✓	851150	187
Re-Power	5e4	40	5.51e−6	39	2.28e−8	✓	848672	188
None	5e5	36	1.10e−6	39	2.35e−8	✓	850835	179
Re-RUC	5e5	36	1.10e−6	41	2.70e−8	✓	851328	181
Re-Power	5e5	36	1.10e−6	39	2.32e−8	✓	849138	178
None	5e6	39	2.46e−8	40	2.59e−8	✓	850817	190
Re-RUC	5e6	39	2.46e−8	38	2.54e−8	✓	851456	188
Re-Power	5e6	39	2.46e−8	41	2.61e−8	✓	848837	193
None	5e7	44	3.45e−9	38	2.38e−8	✓	850980	205
Re-RUC	5e7	44	3.45e−9	40	2.61e−8	✓	851463	208
Re-Power	5e7	44	3.45e−9	39	2.52e−8	✓	849437	207

Table 6 Performance of UC-ER formula on the 118-bus test system based on varying grouping interval widths.

UC Enhanced Round (UC-ER)								
		1st PSLP		2nd PSLP		Results		
Rescale	Inter. width	Iter.	AC-feas.	Iter.	AC-feas.	Feas.	Cost($)	Time (s)
None	0.05	39	2.46e−8	38	2.43e−8	✓	850938	189
Re-RUC	0.05	39	2.46e−8	39	2.53e−8	✓	851503	191
Re-Power	0.05	39	2.46e−8	41	2.61e−8	✓	848837	193
None	0.1	39	2.46e−8	40	2.49e−8	✓	852272	190
Re-RUC	0.1	39	2.46e−8	39	2.53e−8	✓	851503	187
Re-Power	0.1	39	2.46e−8	41	2.61e−8	✓	848837	193
None	0.2	39	2.46e−8	38	7.3e−3	✗	858559	189
Re-RUC	0.2	39	2.46e−8	38	2.53e−8	✓	851772	185
Re-Power	0.2	39	2.46e−8	41	2.56e−8	✓	849525	193

based on the grid numbering system to maintain a structured grouping. The results are detailed in Table 6. We observed that as the interval size increased, the overall robustness of the process decreased. However, since rounding formulas are not optimization approaches, rounding in descending order based on the relaxed commitment value can lead to low-quality, suboptimal solutions. A grouping of the rescaled values with reasonable interval widths in combination with a priority list approach could improve

the quality of the returned solutions in terms of cost minimization (e.g., as in Yang et al. (2014), Senjyu et al. (2003), or Dieu and Ongsakul (2006)).

A detailed comparison between the commitment solutions reported in the literature for UC-ACOPF and UC-DCOPF for the 118-bus test system, and those obtained with our direct relax-and-round strategies, is provided in Table 9 in the Appendix. This comparison shows that our methods yield feasible solutions with costs that are close to published UC-ACOPF results, highlighting their potential as a fast alternative in contexts where AC feasibility is essential.

5 Integrating relax-and-round strategies into a feasibility pump algorithm

The results presented in the previous section correspond to two standard benchmark test systems. The fact that Algorithm 2 succeeds on these instances provides a positive indication that the proposed rescaling and rounding ideas are well grounded. However, in practice, a power system may be stressed (e.g., due to different demand profiles) in such a way that a one-shot direct rounding algorithm may fail to yield a feasible solution. In that case, if Algorithm 2 fails to find a feasible point, the entire strategy fails. This limitation is particularly relevant given the lack of feasibility or optimality guarantees. On the other hand, the literature contains other strategies that, being iterative, can adjust and refine candidate solutions until a satisfactory one is reached. In this context, the rescaling of the relaxed solution and the rounding formulas proposed here can be seen as improved alternatives to standard 0.5 threshold rounding, potentially increasing the success rate of iterative methods that rely on such rounding procedures. In this section, we evaluate the potential of these relax-and-round strategies as drop-in replacements for naive rounding within other iterative heuristics, by integrating them into a Feasibility Pump (FP) algorithm.

The Feasibility Pump method is a heuristic for finding feasible points for MILP problems, first proposed in Fischetti et al. (2005). The core idea of this method is to relax the integrality condition, solve the resulting relaxed problem, and then iteratively solve a family of LP problems until an integer feasible point is found. The formulation of the LP problems retains the original constraints but changes the objective function to be the ℓ_1-norm of the difference between the relaxed solution and its integer-feasible rounded counterpart. To improve the quality of the solutions returned by this heuristic, the so-called Objective Feasibility Pump (OFP) was proposed in Achterberg and Berthold (2007). For an introduction to the method, we refer the reader to the papers cited above. Here, we have implemented an Objective Feasibility Pump algorithm for the Unit Commitment problem with ACPF constraints. More precisely, we extend the work in Li et al. (2024) by considering the minimum up/down constraints in the UC formulation, and by broadening the time horizon to 24 hours. In our case, the FP method is implemented as a heuristic to find feasible points for a MINLP problem with a strong combinatorial nature, involving the solution of a family of non-convex NLP problems. We have implemented the ideas behind the OFP algorithm for the UC-ACOPF problem in a straightforward way. A rigorous adaptation of the FP heuristic to this analytical framework is beyond the scope of this paper; we refer the reader to

D'Ambrosio et al. (2012) for a discussion on extending the FP heuristic to general MINLP problems. The main goal is to use the rescaling strategy and the rounding formulas presented in the previous section together with our implementation of the FP method to check if the performance of the heuristic improves, compared to using the standard FP algorithm in the literature.

Let us consider the vector $\boldsymbol{u}^{\text{in}}$, consisting of binary values $u^{\text{in}}_{g,t}$ for each g in the set of thermal generators G_{th} and each time period $t \in T$. Each value $u^{\text{in}}_{g,t}$ corresponds specifically to the decision variable $\tilde{u}_{g,t}$ of the problem RUC-ACOPF, grouped in a vector denoted by $\tilde{\boldsymbol{u}}$. The ℓ_1-norm of the difference between $\boldsymbol{u}^{\text{in}}$ and $\tilde{\boldsymbol{u}}$ can be computed as

$$\|\boldsymbol{u}^{\text{in}} - \tilde{\boldsymbol{u}}\|_{\ell_1} = \sum_{(g,t)\in G_{\text{th}}\times T} \left| u^{\text{in}}_{g,t} - \tilde{u}_{g,t} \right| = \sum_{t\in T} \sum_{g\in G_{\text{th}}} \left| u^{\text{in}}_{g,t} - \tilde{u}_{g,t} \right|.$$

Since $\boldsymbol{u}^{\text{in}}$ is a vector of binary variables, the previous formula can also be expressed as

$$\|\boldsymbol{u}^{\text{in}} - \tilde{\boldsymbol{u}}\|_{\ell_1} = \sum_{(g,t)\in G_{\text{th}}\times T : u^{\text{in}}_{g,t}=0} \tilde{u}_{g,t} + \sum_{(g,t)\in G_{\text{th}}\times T : u^{\text{in}}_{g,t}=1} \left(1 - \tilde{u}_{g,t}\right).$$

The cost function for the sequence of NLP problems iteratively solved in the objective feasibility pump algorithm is defined through a convex combination of the UC cost function f_{UC} and the ℓ_1-norm difference between the integer and relaxed decision variables. Thus:

$$f_{\text{FP}}(\boldsymbol{x}, \boldsymbol{y}) := \frac{1-\alpha}{W_{\ell_1}} \|\boldsymbol{u}^{in} - \tilde{\boldsymbol{u}}\|_{\ell_1} + \frac{\alpha}{W_{\text{UC}}} f_{\text{UC}}(\boldsymbol{x}, \boldsymbol{y}), \tag{19}$$

where W_{ℓ_1} and W_{UC} are weights used to normalize the difference in magnitude between the two terms of the cost function, and the convex combination factor $\alpha \in (0, 1)$ is updated after each iteration.

Let us consider the set of NLP problems denoted as [FP-RUC], parameterized by $\boldsymbol{u}^{in}$ and α:

$$\text{[FP-RUC]}\left(\boldsymbol{u}^{in}, \alpha\right) \begin{cases} \min\ (19), \\ \text{s.t.: } (2) - (14), \\ \quad V_{i,t} \in \left[V_{\min,i}, V_{\max,i}\right],\ \theta_{i,t} \in [-\pi, \pi],\ i \in I, t \in T, \\ \quad \theta_{i,t} = \theta_{i,0},\ \forall t \in T,\ \text{ for the reference node}, \\ \quad Q^{\text{G}}_{g,t} \in \left[Q_{\min,g}, Q_{\max,g}\right],\ \forall (g,t) \in G_{\text{sc}} \times T, \\ \quad P^{\text{G}}_{g,t} \in \left[0, P_{\max,g}\right],\ \forall (g,t) \in G_{\text{th}} \times T, \\ \quad Q^{\text{G}}_{g,t} \in \left[\min\{Q_{\min,g}, 0\}, \max\{Q_{\max,g}, 0\}\right],\ \forall (g,t) \in G_{\text{th}} \times T, \\ \quad P^{\text{res}}_{g,t} \in \left[0, P_{\max,g} - P_{\min,g}\right],\ \forall (g,t) \in G_{\text{th}} \times T, \\ \quad u_{g,t}, v_{g,t}, w_{g,t} \in [0,1],\ \forall (g,t) \in G_{\text{th}} \times T. \end{cases} \tag{20}$$

Each distinct pair of values for $\left(\boldsymbol{u}^{in}, \alpha\right)$ defines a unique problem instance within this family. Our relax-and-round approach using the FP heuristic is described in Algorithms 3 and 4.

Algorithm 3 Relax-and-round with Feasibility Pump

1: Consider [UC-AC].
2: Solve [RUC-AC]. Let $\tilde{u}_{g,t}$ be the relaxed commitment.
3: Round $\tilde{u}_{g,t}$ values to obtain $\boldsymbol{u}^{in}$
4: Apply Algorithm 4 implementing the Feasibility Pump using $\boldsymbol{u}^{in}$ as the initial integer vector.

Algorithm 4 Feasibility Pump algorithm

Require: [UC-AC] problem data, $\boldsymbol{u}^{\text{in}}$ initial integer value, and parameters: *maxit*, *maxrst*, α_0, φ_α, δ_α and S.
1: Initialize: $rst = 0$, $\boldsymbol{u}_0^{\text{in}} = \boldsymbol{u}^{\text{in}}$.
2: **for** $k \leftarrow 1$ **to** *maxit* **do**
3: Solve [FP-RUC]$\left(\boldsymbol{u}_{k-1}^{\text{in}}, \alpha_{k-1}\right)$. Let $\left(\hat{\boldsymbol{x}}_k, \hat{\boldsymbol{y}}_k\right)$ be the solution, and $\hat{\boldsymbol{u}}_k$ the relaxed commitment.
4: **if** $\hat{\boldsymbol{u}}_k$ is integer **then**
5: **Return** $\left(\hat{\boldsymbol{x}}_k, \hat{\boldsymbol{y}}_k\right)$ and **End**.
6: **else**
7: Round $\hat{\boldsymbol{u}}_k$ to obtain $\boldsymbol{u}_k^{\text{in}}$.
8: **end if**
9: **if** $\left(\boldsymbol{u}_k^{\text{in}}, \alpha_k\right)$ is a stationary point **then**
10: Apply a flip to the binary values of S random components of $\boldsymbol{u}_k^{\text{in}}$, and $rst = rst + 1$.
11: **if** $rst >$ *maxrst* **Exit for, go to 15:**
12: **end if**
13: Update: $\alpha_k = \alpha_{k-1}\varphi_\alpha$.
14: **end for**
15: Choose $\left(\hat{\boldsymbol{x}}_h, \hat{\boldsymbol{y}}_h\right)$, $h \in \{1, \ldots, k\}$, with closest $\hat{\boldsymbol{u}}_h$ to its projection in **7:** in the ℓ_1-norm sense.
16: Round $\hat{\boldsymbol{u}}_h$ and construct $\boldsymbol{y}_h^{\text{in}}$.
17: Fix $\boldsymbol{y}_h^{\text{in}}$ in [UC-AC], and solve the resulting problem [ACOPF]. Let $\boldsymbol{x}_{\text{AC}}$ be the solution.
18: **Return** $\left(\boldsymbol{x}_{\text{AC}}, \boldsymbol{y}_h^{in}\right)$ and **End**.

Let us now discuss the specifics of Algorithm 4. After solving [FP-RUC]$\left(\boldsymbol{u}_{k-1}^{\text{in}}, \alpha_{k-1}\right)$ at iteration k, we denote by $\hat{\boldsymbol{u}}_k$ the values for the relaxed unit commitment in the solution. In lines 4-8 of the algorithm, if $\hat{\boldsymbol{u}}_k$ is an integer vector, we declare that the pair $\left(\hat{\boldsymbol{x}}_k, \hat{\boldsymbol{y}}_k\right)$ is a feasible point for the UC-ACOPF problem and the algorithm finishes; otherwise, we round $\hat{\boldsymbol{u}}_k$ to obtain the next candidate for the integer commitment, $\boldsymbol{u}_k^{\text{in}}$. Notice that the solution of each problem [FP-RUC] $\left(\boldsymbol{u}_{k-1}^{\text{in}}, \alpha_{k-1}\right)$ can coincide with the integer vector $\boldsymbol{u}_{k-1}^{\text{in}}$ in the corresponding relaxed components only if the combinatorial constraints of the UC problem are satisfied. If the newly obtained integer vector $\boldsymbol{u}_k^{\text{in}}$ matches any previously obtained integer solution, say $\boldsymbol{u}_{\tilde{k}}^{\text{in}}$ for some earlier iteration $\tilde{k} < k$ while also satisfying $\alpha_{\tilde{k}} - \alpha_k \leq \delta_\alpha$ we consider the pair $\left(\boldsymbol{u}_k^{\text{in}}, \alpha_k\right)$ to be a stationary point for the algorithm. To prevent the algorithm from proceeding iteratively while returning the same value for the integer variables, after rounding $\hat{\boldsymbol{u}}_k$

we verify if a stationary point is reached, in which case we apply a perturbation to $\boldsymbol{u}_k^{\text{in}}$ by flipping the binary values of S random components. This perturbation mechanism can be seen as a 'reset', as we also update $\alpha_k = \alpha_0/(rst + 1)$, where rst counts the number of resets, thereby partially restarting the algorithm with different parameters. To prevent excessive resets, we set a maximum number, $maxrst$, as an early stopping criterion. The rounding procedure described in Algorithm 3 (step 2) and Algorithm 4 (lines 7 and 16) are independent. This means any rescaling and rounding formula combinations, as presented in the previous sections, can be applied. The naive rounding formula with no rescale (None+NR) projects the relaxed solution to the nearest integer vector in the ℓ_1-norm sense. However, not all these integer combinations are feasible under the UC problem constraints, highlighting the importance of combining these techniques effectively for better solution feasibility and quality. In this sense, we expect that our proposed rescaling+rounding formulas provide a more accurate direct approximation of the projection of $\hat{\boldsymbol{u}}_k$ in the UC skeleton solution space.

In the following, we present the results of the FP algorithm applied to the 6-bus and the 118-bus test systems. To solve the non-convex NLP problems, we once again employed the PSLP method. For both problems [RUC-AC] and [ACOPF], a penalty weight of 5e6 was used, whereas for problem [FP-RUC], the penalty weight was set to 500. Furthermore, the parameters for the cost function were defined as follows: we set $W_{\ell_1} = t_f\,|G_{\text{th}}|$ and $W_{\text{UC}} = t_f\,|G_{\text{th}}|\max_{g\in G_{\text{th}}}\{a_{g,2}\}$, where $|G_{\text{th}}|$ denotes the number of thermal generators in the system.

For the FP algorithm, we used the following parameter settings: $maxrst = 3$, $\alpha_0 = 0.75$, $\varphi_\alpha = 0.5$, and $\varphi_\beta = 0.075$. The parameter S was chosen as a percentage of $t_f\,|G_{\text{th}}|$, and the results for values corresponding to its 10%, 25%, 50%, 75%, and 100% were compared. The value 100% corresponds to the total number of relaxed variables that must be rounded for the problem. The larger the value of S, the more we rely on random perturbations as a multi-start mechanism. As we will show, different values for S yield varying performance depending on the combination of the rescaling approach and rounding formula used.

The performance results of the FP algorithm for both test systems are summarized in Tables 7 and 8. It should be noted that the parameter S introduces stochasticity into the results of the algorithm. Each configuration for parameter S was tested 10 times, with the reported statistics reflecting the range of values obtained. In both cases, step 2 of Algorithm 3 applies the NR formula without rescaling, initializing the FP algorithm with a non-feasible integer solution (see Tables 2 and 4). The % column reports the success rate, defined as the percentage of runs in which the algorithm returned a feasible point, with respect to the total number of executions.

For the 6-bus test system, the None+NR rounding approach produced infeasible solutions in 90% of the cases. Notably, for the remaining 10%, the algorithm required two restarts to obtain a feasible solution. In contrast, when using Re-RUC+NR with $S = t_f\,|G_{\text{th}}|$, a feasible solution was found after only one restart, yielding a different feasible solution in each experiment. As the value of S decreased, the Re-RUC+NR approach had increasing difficulty in identifying feasible solutions. Finally, the Re-RUC+UC-ER method achieved convergence in only two iterations, eliminating the need for any random perturbations. Notice that the operating costs of the feasible points returned by the FP algorithm are generally higher than those in Table 3. This

Table 7 Summary of the FP algorithm performance for the 6-bus test system example.

6-bus test system								
Feasibility Pump				PSLPs		Results		
Rescale+Round	S	Iter.	rst	Total iter.	Feas.	Cost($)	Time (s)	%
None+NR	7	13-15	3	312 – 377	✗	94704 – 99641	38 – 48	0%
	18	15	3	397 – 412	✗	94704 – 102115	48 – 51	0%
	36	12	2	288	✓	105701	35	10%
	54	11	2	266	✓	107801	32	10%
	72	15	3	394 – 418	✗	94704 – 104999	47 – 51	0%
Re-RUC+NR	7	7-16	1-3	186 – 470	✓	102485 – 103516	22 – 57	80%
	18	7-11	1-2	184 – 313	✓	103264 – 105640	22 – 38	90%
	36	7	1	186 – 190	✓	104014 – 106166	22 – 23	100%
	54	7-11	1-2	183 – 319	✓	106240 – 107439	22 – 38	100%
	72	7	1	184 – 191	✓	106698 – 108507	22 – 23	100%
Re-RUC+UC-ER	Any	2	0	37	✓	102146	5	100%

Table 8 Summary of the FP algorithm performance for the 6-bus test system example.

118-bus test system							
Feasibility Pump		PSLPs	Feasibility		Results		
Rescale+Round	S	Total iter.	AC	UC	Cost($)	Time (s)	%
None+NR	324	799	1e−5	✓	929131	4188	10%
Re-RUC+NR	130	1006	1e−5	✓	871041 – 871746	3524	10%
	324	520 – 560	1e−5	✓	871041 – 871746	2204 – 2320	30%
	648	3817	1e−5	✓	907184	15381	10%
Re-RUC+UC-ER	324	720 – 2206	1e−5	✓	873450 – 892570	3177 – 6554	30%
	648	2125 – 6367	1e−5	✓	889443 – 911307	5721 – 14747	40%
	972	400 – 2084	1e−5	✓	899136 – 920748	1754 – 14391	60%
	1296	360 – 2620	1e−5	✓	899924 – 929276	1584 – 3120	100%

is expected because FP minimizes the composite objective (19), which includes an ℓ_1-proximity term and is primarily designed to recover feasibility rather than just UC cost optimality.

For the 118-bus test system, we report only the feasible points obtained for the different values of S and for each combination of rescaling and rounding strategies. The larger size of this test system made it challenging to fine-tune the parameters for both the PSLP and FP algorithms. This may be related to the numerical conditioning of the linear programming problems iteratively solved, and could be addressed in future work. For completeness, we adopted a higher feasibility threshold of 1e−5 for this test system. The None+NR approach did not consistently yield feasible solutions for any value of S, except for a single feasible solution found for $S = t_f\,|G_{\text{th}}|\,0.5$. The Re-RUC+NR and Re-RUC+UC-ER approaches showed contrasting performance trends based on the value of S. For Re-RUC+UC-ER, using $S = t_f\,|G_{\text{th}}|$ yielded the best

results, achieving a feasibility rate of 100% within the set tolerance. As S decreased, the feasibility rate for Re-RUC+UC-ER gradually decreased to 30% at $S = t_f\ |G_{\text{th}}|\ 0.25$. Conversely, Re-RUC+NR performed better for smaller values of S, also achieving 30% feasibility at $S = t_f\ |G_{\text{th}}|\ 0.25$, but showing reduced performance for other S. For smaller values of S, none of the rescaling and rounding combinations produced feasible points. This behavior aligns with previous findings on the usefulness of a multi-start mechanism in FP implementations for MINLP problems, as reported in D'Ambrosio et al. (2012).

6 Conclusions

Finding feasible solutions to the UC problem with ACPF constraints remains a significant challenge due to its combinatorial complexity and non-convex nature. Many existing heuristics address this problem by relaxing the integrality of the commitment variables and subsequently applying rounding strategies. In this work, we introduce two novel heuristics that aim to improve relax-and-round strategies. The first heuristic applies a physics-based rescaling to the relaxed commitment variables before rounding, while the second proposes an improved rounding formula that ensures combinatorial feasibility and better preserves active power balance in the system.

Both heuristics were evaluated in a direct relax-and-round framework on the 6-bus and 118-bus test systems. The results show that our approach provides a viable alternative for efficiently obtaining AC-feasible solutions. Furthermore, integrating these heuristics into the Feasibility Pump algorithm confirms their applicability for improving other approaches in the literature that depend on heuristic rounding methods. Compared to standard rounding, where no rescaling is applied and rounding is performed around the 0.5 threshold, our heuristics consistently produced more feasible solutions for the UC-ACOPF problem and improved convergence rates.

The non-convex NLPs arising in both algorithms were solved locally using the PSLP method, with the solution times primarily influenced by the PSLP convergence behavior. Future work could improve the performance of these methods by using more robust or ad hoc solvers for the ACOPF problems. Additionally, exploring global optimization techniques could be a promising direction for further research.

Appendix A

Nomenclature

$a_{g,2}, a_{g,1}, a_{g,0}$	coefficients of the quadratic cost function for generation unit g
a_{il}	coefficient il of matrix $\mathcal{A}$
$\mathcal{A}$	incidence matrix of $\mathcal{P}$
b_{ik}	imaginary part of coefficient ik of admittance matrix $\mathbb{Y}$
$c_{g,u}, c_{g,d}$	start-up/shut-down constant costs of generation unit g
$c_{1,il}, c_{2,il}$	coefficient il of matrices C_1,C_2
C_1, C_2	auxiliary matrices defined from $\mathcal{A}$
g	generation unit index

g_{ik}	real part of coefficient ik of admittance matrix $\mathbb{Y}$
G	set of generation units
G_i	set of generation units placed at bus i
G_r	set of generation units in region r
G_{th}	set of thermal generation units
G_{sc}	set of synchronous condensers
i	bus index
I	set of buses
I_D	set of buses where power is demanded
l	line index
L	set of lines
N_{b}	number of buses
N_{l}	number of elements
$\mathcal{N}(i)$	set of bus i neighbors
$\mathcal{P}$	directed graph modeling the power grid
$P^{\text{G}}_{g,t}$	active power generated by generation unit g at time t
$\tilde{P}^{\text{G}}_{g,t}$	relaxation of $P^{\text{G}}_{g,t}$ to $\left[0, P_{\max,g}\right]$
$P^{D}_{i,t}$	active power demand at bus i at time t
$P_{\max,g}$, $P_{\min,g}$	maximum/minimum active power generation limits for generation unit g
$P^{\text{res}}_{g,t}$	active power reserve for generation unit g at time t
$P^{\text{res}}_{r,t}$	active power reserve requirements for region r at time t
$Q^{\text{G}}_{g,t}$	reactive power generated by generation unit g at time t
$\tilde{Q}^{\text{G}}_{g,t}$	relaxation of $Q^{\text{G}}_{g,t}$ to $\left[\min\{Q_{\min,g}, 0\}, \max\{Q_{\max,g}, 0\}\right]$
$Q^{D}_{i,t}$	reactive power demand at bus i at time t
$Q_{\max,g}$, $Q_{\min,g}$	maximum/minimum reactive power generation limits for generation unit g
r	region index
R	set of regions
R^{d}_{g}, R^{u}_{g}	active power ramp down/up specifications for generation unit g
S^{d}_{g}, S^{u}_{g}	shutting-down/starting-up active power generation limits of generation unit g
$\vec{\mathbb{S}}$	vector of complex power injections from the buses to the grid
t	time index
T	set of discrete times
T^{d}_{g}, T^{u}_{g}	minimum down/up times for generation unit g
$u_{g,t}$	on/off status of generation unit g at time t
$\tilde{u}_{g,t}$	continuous relaxation of $u_{g,t}$ to [0, 1]
$v_{g,t}$	turn on decision variable for generation unit g at time t
$\tilde{v}_{g,t}$	continuous relaxation of $v_{g,t}$ to [0, 1]
$V_{i,t}$	complex voltage magnitude of bus i at time t
$V_{\max,i}$, $V_{\min,i}$	maximum/minimum complex voltage magnitude limits for bus i
$\vec{\mathbb{V}}$	vector of complex voltage for the buses
$w_{g,t}$	turn off decision variable for generation unit g at time t

$\tilde{w}_{g,t}$	continuous relaxation of $w_{g,t}$ to [0, 1]
$\mathbb{Y}$	admittance matrix of the power grid
$\mathbb{Y}_1$, $\mathbb{Y}_2$	from/to components of the admittance matrix $\mathbb{Y}$
$\vec{\mathbb{Y}}_{\text{sh}}$	complex vector of bus shunt elements
$\theta_{i,t}$	complex voltage angle of bus b at time t

Appendix B

Table 9 presents a comparison between the commitment solutions reported in the literature for the UC-ACOPF and UC-DCOPF problems and those obtained with our direct relax-and-round strategies. All commitments were selected from the experiments with a penalty weight of 5e6, ensuring UC-ACOPF feasibility. The rescale-and-round strategies generally produced more committed units than the optimization approaches over the binary decision variables in Castillo et al. (2016) and Liu et al. (2018). In principle, de-commitment heuristics such as those proposed by Borghetti et al. (2003) could be applied to address this issue, although maintaining AC feasibility may be challenging in highly constrained grids. The lowest-cost solution was obtained with the Re-Power rescaling combined with the NR formula, but this approach showed limited robustness across experiments in terms of feasibility, as discussed in Section 4.2. Compared with the local solution in Castillo et al. (2016), our cost differences remained below 10000, while UC-DCOPF underestimated the cost by more than 20000. These results show that, although our method is not a full optimization heuristic, it provides a fast alternative for applications where AC feasibility is a priority.

Table 9 Comparison between commitment and cost solutions for the 118-bus test system.

	UC-DCOPF	Literature UC-ACOPF		Direct strategies				
	Castillo et al. (2016)	Liu et al. (2018) Global	Castillo et al. (2016) Local	NR			UC-ER	
Cost ($)	814715	835926	843591	Re-RUC 847740	Re-Power 846543	None 850817	Re-RUC 851456	Re-Power 848837
g.u. 1	–	–	–	–	–	–	–	–
g.u. 2	–	–	–	–	–	–	–	–
g.u. 3	–	–	–	1–24	9–23	1–24	1–24	9–10,18
g.u. 4	1–24	1–10,24	1–24	1–24	1–24	1–24	1–24	1–24
g.u. 5	1–24	1–24	1–24	1–24	1–24	1–24	1–24	1–24
g.u. 6	–	–	–	–	–	–	–	–
g.u. 7	–	11–22	10–23	6–24	6–24	7–23	7–23	7–23
g.u. 8	–	–	–	–	–	–	–	–
g.u. 9	–	–	–	–	–	–	–	–
g.u. 10	1–24	1–2,12–24	1–24	1–24	1–24	1–24	1–24	1–24
g.u. 11	1–24	1–24	1–24	1–24	1–24	1–24	1–24	1–24
g.u. 12	–	–	–	–	–	–	–	–
g.u. 13	–	–	–	–	–	–	–	–
g.u. 14	–	10–22	9–22	8–24	8–24	8–24	8–24	8–24
g.u. 15	–	–	–	–	–	–	–	–
g.u. 16	10–18	9–16	10–23	8–24	8–24	8–24	8–23	8–23
g.u. 17	–	–	–	–	–	–	–	–
g.u. 18	–	–	–	–	–	–	–	–
g.u. 19	–	–	–	10–22	10–22	9–14	8–15	8–15
g.u. 20	1–24	1–24	1–24	1–24	1–24	1–24	1–24	1–24
g.u. 21	–	8–24	8–24	1–24	1–24	1–24	1–24	1–24
g.u. 22	–	–	–	9–23	9–23	9–19	9–22	9–22

Table 9 continued

	UC-DCOPF	Literature UC-ACOPF		Direct strategies				
	Castillo et al. (2016)	Liu et al. (2018)	Castillo et al. (2016)	NR			UC-ER	
		Global	Local	Re-RUC	Re-Power	None	Re-RUC	Re-Power
Cost ($)	814715	835926	843591	847740	846543	850817	851456	848837
g.u. 23	–	–	–	–	–	–	–	–
g.u. 24	–	9–23	9–23	7–24	7–24	7–24	7–24	7–24
g.u. 25	10–22	–	–	1–24	1–24	1–24	1–23	1–23
g.u. 26	–	–	–	–	–	–	–	––
g.u. 27	1–24	1–2,13–24	1–24	1–24	1–24	1–24	1–24	1–24
g.u. 28	1–24	1–24	1–24	1–24	1–24	1–18	1–24	1–24
g.u. 29	1–24	1–24	1–24	1–24	1–24	1–24	1–24	1–24
g.u. 30	8–23	1––24	7–24	1–24	1–24	1–24	1–24	1–24
g.u. 31	–	–	–	–	–	–	–	–
g.u. 32	–	–	–	–	–	–	–	–
g.u. 33	–	–	–	–	–	–	–	–
g.u. 34	7–24	7–24	7–24	1–24	1–24	1–24	1–24	1–24
g.u. 35	1–24	1–24	1–24	1–24	1–24	1–24	1–24	1–24
g.u. 36	1–24	1–24	1–24	1–24	1–24	1–24	1–24	1–24
g.u. 37	1–24	8–23	11–17	1–24	1–24	1–24	1–24	1–24
g.u. 38	–	–	–	8,17–28	8,17–18	8–9,18	8–9,18	8–10,18
g.u. 39	1–24	–	1–24	–	–	18–24	18–24	18–24
g.u. 40	1–24	1–10,22–24	1–24	1–24	1–24	1–24	1–24	1–24
g.u. 41	–	–	–	–	–	–	–	–

Table 9 continued

	UC-DCOPF	Literature UC-ACOPF		Direct strategies				
	Castillo et al. (2016)	Liu et al. (2018)	Castillo et al. (2016)	NR		UC-ER		
Cost ($)	814715	Global 835926	Local 843591	Re-RUC 847740	Re-Power 846543	None 850817	Re-RUC 851456	Re-Power 848837
g.u. 42	–	–	–	–	–	–	–	–
g.u. 43	9–24	1–24	10–23	1–24	1–24	1–24	1–24	1–24
g.u. 44	–	–	–	–	–	10–17	10–17	10–17
g.u. 45	1–24	1–24	1–24	1–24	1–24	1–24	1–24	1–24
g.u. 46	–	–	–	–	––	–	–	–
g.u. 47	–	–	–	–	–	–	–	–
g.u. 48	–	–	–	8–23	8–23	8–23	8–23	8–23
g.u. 49	–	–	–	–	–	–	–	–
g.u. 50	–	–	–	–	–	–	–	–
g.u. 51	–	9–13	9–24	8–23	8–23	8–12,18–22	8–22	8–22
g.u. 52	–	14–23	–	8–24	8–24	8–23	8–23	8–23
g.u. 53	8–24	7–24	1–24	1–24	1–24	1–24	1–24	1–24
g.u. 54	9–23	9–23	9–20	9–23	9–23	8–23	9–23	9–23

Acknowledgements This work was partially supported by MCIN /AEI /10.13039/501100011033 / FEDER, UE through grant PID2021-122625OB-I00, by Ministerio de Ciencia, Innovación y Universidades through the Plan Nacional de I+D+i (MTM2017-86459-R) and the grant PRE2018-083893, and by Xunta de Galicia funds through grant GRC GI-1563 - ED431C 2025/09. and. It has also been supported by the German Research Foundation (DFG) under grant GO 1920/11-1 and 12-1.

Author Contributions All authors (D.G., S.G.,A.R.,P.S.) contributed to the conceptualization, formal analysis, methodology, writing, and review of the manuscript. Additionally, A.R. conducted the numerical simulations.

Funding Open Access funding enabled and organized by Projekt DEAL. Open Access funding enabled and organized by Projekt DEAL.

Data Availability No datasets were generated or analysed during the current study.

Declarations

Competing interests The authors declare no competing interests.

References

Achterberg T (2009) SCIP: solving constraint integer programs. Math Program Comput 1(1):1–41

Achterberg T, Berthold T (2007) Improving the feasibility pump. Discret Optim 4(1):77–86

Aharwar A, Naresh R, Sharma V, Kumar V (2023) Unit commitment problem for transmission system, models and approaches: A review. Electric Power Systems Research 223:109671

Anjos MF, Conejo AJ, et al (2017) Unit commitment in electric energy systems. Foundations and Trends® in Electric Energy Systems, 1 (4): 220–310,

Atakan S, Lulli G, Sen S (2017) A state transition mip formulation for the unit commitment problem. IEEE Trans Power Syst 33(1):736–748

Bai X, Wei H (2009) Semi-definite programming-based method for security-constrained unit commitment with operational and optimal power flow constraints. IET Generation Transmission & Distribution 3(2):182–197

Bai Y, Zhong H, Xia Q, Kang C, Xie L (2015) A decomposition method for network-constrained unit commitment with AC power flow constraints. Energy 88:595–603

Bazaraa MS, Sherali HD, Shetty CM (2006) Nonlinear programming: theory and algorithms. John Wiley & Sons,

Belotti P, Kirches C, Leyffer S, Linderoth J, Luedtke J, Mahajan A (2013) Mixed-integer nonlinear optimization. Acta Numer 22:1–131

Borghetti A, Frangioni A, Lacalandra F, Nucci CA (2003) Lagrangian heuristics based on disaggregated bundle methods for hydrothermal unit commitment. IEEE Trans Power Syst 18(1):313–323

Carøe CC, Schultz R (1998) A two-stage stochastic program for unit commitment under uncertainty in a hydro-thermal power system. Preprint SC 98–11,

Carrión M, Arroyo JM (2006) A computationally efficient mixed-integer linear formulation for the thermal unit commitment problem. IEEE Trans Power Syst 21(3):1371–1378

Castillo A, Laird C, Silva-Monroy CA, Watson J-P, O'Neill RP (2016) The unit commitment problem with AC optimal power flow constraints. IEEE Trans Power Syst 31(6):4853–4866

Chen H, Liu M, Cheng Y, Lin S (2019) Modeling of unit commitment with AC power flow constraints through semi-continuous variables. IEEE Access 7:52015–52023
Constante-Flores GE, Conejo AJ, Qiu F (2022) AC network-constrained unit commitment via conic relaxation and convex programming. International Journal of Electrical Power & Energy Systems 134:107364
Czyzyk J, Mesnier MP, Moré JJ (1998) The NEOS server. IEEE Journal on Computational Science and Engineering 5(3):68–75
Dieu V, Ongsakul W (2006) Enhanced augmented lagrangian hopfield network for unit commitment. IEE Proceedings-Generation Transmission and Distribution 153(6):624–632
D'Ambrosio C, Frangioni A, Liberti L, Lodi A (2012) A storm of feasibility pumps for nonconvex minlp. Math Program 136:375–402
Fischetti M, Glover F, Lodi A (2005) The feasibility pump. Math Program 104:91–104
Fu Y, Shahidehpour M, Li Z (2005) Security-constrained unit commitment with AC constraints. IEEE Trans Power Syst 20(3):1538–1550
Fu Y, Shahidehpour M, Li Z (2006) AC contingency dispatch based on security-constrained unit commitment. IEEE Trans Power Syst 21(2):897–908
Gao L, Fang J, Ai X, Wei L, Cui S, Yao W, Wen J (2024) A topology-guided learning framework for security-constraint unit commitment. Available at SSRN 4718365,
Gurobi Optimization, LLC. Gurobi Optimizer Reference Manual, 2023. https://www.gurobi.com
He C, Wu L, Liu T, Shahidehpour M (2016) Robust co-optimization scheduling of electricity and natural gas systems via admm. IEEE Transactions on Sustainable Energy 8(2):658–670
Kjeldsen NH, Chiarandini M (2012) Heuristic solutions to the long-term unit commitment problem with cogeneration plants. Computers & Operations Research 39(2):269–282
Lazić J (2016) Variable and single neighbourhood diving for mip feasibility. Yugoslav Journal of Operations Research, 26 (2),
Li P, Su J, Bai X (2024) An objective feasibility pump method for optimal power flow with unit commitment variables. Electric Power Systems Research 236:110928
Liu J, Laird CD, Scott JK, Watson J-P, Castillo A (2018) Global solution strategies for the network-constrained unit commitment problem with AC transmission constraints. IEEE Trans Power Syst 34(2):1139–1150
Ma Z, Zhong H, Xia Q, Kang C, Wang Q, Cao X (2020) A unit commitment algorithm with relaxation-based neighborhood search and improved relaxation inducement. IEEE Trans Power Syst 35(5):3800–3809
Montero L, Bello A, Reneses J (2022) A review on the unit commitment problem: Approaches, techniques, and resolution methods. Energies 15(4):1296
Morales-España G, Latorre JM, Ramos A (2013) Tight and compact milp formulation for the thermal unit commitment problem. IEEE Trans Power Syst 28(4):4897–4908
Murillo-Sanchez CE, Thomas RJ (2000) Parallel processing implementation of the unit commitment problem with full AC power flow constraints. In Proceedings of the 33rd Annual Hawaii International Conference on System Sciences, pages 9-pp. IEEE,
Najman J, Bongartz D, Sass S, Djelassi H, Jungen D, Huster WR, Burre J, Karacasulu K, Schweidtmann AM, Mitsos A (2019) Mccormick-based algorithm for mixed-integer nonlinear global optimization. In 2019 AIChE Annual Meeting. American Institute of Chemical Engineers,
Nick M, Alizadeh-Mousavi O, Cherkaoui R, Paolone M (2015) Security constrained unit commitment with dynamic thermal line rating. IEEE Trans Power Syst 31(3):2014–2025
Ordoudis C, Pinson P, Zugno M, Morales JM (2015) Stochastic unit commitment via progressive hedging-extensive analysis of solution methods. In 2015 IEEE Eindhoven PowerTech, pages 1–6. IEEE,
Ostrowski J, Anjos MF, Vannelli A (2011) Tight mixed integer linear programming formulations for the unit commitment problem. IEEE Trans Power Syst 27(1):39–46
Padhy NP (2004) Unit commitment-a bibliographical survey. IEEE Trans Power Syst 19(2):1196–1205
Sauer W (2014) Uplift in rto and iso markets. Tech. Rep, Federal Energy Regulatory Commission
Sawa T, Sato Y, Tsurugai M, Onishi T (2007) Security constrained integrated unit commitment using quadratic programming. In 2007 IEEE Lausanne Power Tech, pages 1858–1863. IEEE,
Senjyu T, Shimabukuro K, Uezato K, Funabashi T (2003) A fast technique for unit commitment problem by extended priority list. IEEE Trans Power Syst 18(2):882–888
Tejada-Arango DA, Lumbreras S, Sánchez-Martín P, Ramos A (2019) Which unit-commitment formulation is best? A comparison framework. IEEE Trans Power Syst 35(4):2926–2936

Tejada-Arango DA, Wogrin S, Sánchez-Martın P, Ramos A. Unit commitment with ACOPF constraints: Practical experience with solution techniques. 2019 IEEE Milan PowerTech, pages 1–6, (2019b)
Tuncer D, Kocuk B (2022) An misocp-based decomposition approach for the unit commitment problem with AC power. IEEE Trans Power Syst 38(4):3388–3400
Wang Z, Wang L, Li Z, Cheng X, Li Q (2021) Optimal distributed transaction of multiple microgrids in grid-connected and islanded modes considering unit commitment scheme. International Journal of Electrical Power & Energy Systems 132:107146
Wu J, Luh PB, Chen Y, Yan B, Bragin MA (2023) Synergistic integration of machine learning and mathematical optimization for unit commitment. IEEE Trans Power Syst 39(1):391–401
Wuijts RH, van den Akker M, van den Broek M (2024) Effect of modelling choices in the unit commitment problem. Energy Systems 15(1):1–63
Xavier ÁS, Qiu F, Ahmed S (2021) Learning to solve large-scale security-constrained unit commitment problems. INFORMS J Comput 33(2):739–756
Yang L, Jian J, Zhu Y, Dong Z (2014) Tight relaxation method for unit commitment problem using reformulation and lift-and-project. IEEE Trans Power Syst 30(1):13–23
Zhang Z, Liu M, Xie M, Dong P (2023) A mathematical programming-based heuristic for coordinated hydrothermal generator maintenance scheduling and long-term unit commitment. International Journal of Electrical Power & Energy Systems 147:108833
Zimmerman RD, Murillo-Sánchez C (2020) Matpower user's manual. 2024. https://matpower org/docs/MATPOWER-manual. pdf. Accessed, 27,